V International Conference on Computational Methods in Marine Engineering
MARINE 2013
B. Brinkmann and P. Wriggers (Eds)

INFLUENCE OF PROPELLER TIP ROUGHNESS ON TIP VORTEX STRUCTURE - MARINE 2013

Christian Krueger*, Nikolai Kornev*, Christian Semlow† Matthias Paschen†

*Chair of Modelling and Simulation (LEMOS)
University of Rostock (URO)
Albert-Einstein-Str. 2, 18059 Rostock, Germany
e-mail: christian.krueger@uni-rostock.de, web page: http://www.lemos.uni-rostock.de/

† Chair of Ocean Engineering (LMT)
University of Rostock (URO)
Albert-Einstein-Str. 2, 18059 Rostock, Germany
e-mail: christian.semlow@uni-rostock.de - Web page: http://www.lmt.uni-rostock.de

Key words: Tip Vortex Cavitation, Marine Propellers

Abstract. This paper investigates the effects of propeller tip roughness on the tip vortex formation. It was shown, that sand grain roughness can lead to a significant drop in angular vortex momentum and therefore reduced vortex vacuum. Due to additional viscous stresses between propeller blade and detached tip vortex, the momentum is transformed into turbulent kinetic energy. As the turbulent scales are dissipated partly, the energy content of the system is reduced. This effect shows to be sensitive to application area and roughness height.

1 INTRODUCTION

Modern shipbuilding and development shows a strong demand for highly efficient and powerful propulsion systems. Moreover, tendencies of maximizing the cargo hold lead to decreasing space provided for the propulsion system. On the downside of this progression are highly tip-loaded propellers. This can lead to prominent tip vortex structures and subsequently forwarding to frequent tip vortex cavitation, hull excitation and rudder erosion.

Within a joint research project of MMG Waren GmbH and the University of Rostock an innovative approach has been investigated claiming the possibility of pertubating propeller tip vortices by a roughened propeller tip region.

2 THEORETICAL BACKGROUND

In marine propulsion tip vortices come to mind especially when showing up in its extreme occurrence, forming a cavitating vortex helix. Even though erosion, induced by tip vortex cavitation, in general does not impact on the propeller itself, the harmful effects on installations placed downstream like rudders are quite remarkable [3]. Furthermore, the comfort conditions are affected as well. Hull excitation and underwater noise [10], arising from increased 2^{nd} order pressure fluctuations, are challenges of modern propeller design.

The approach, for delaying or modifying tip vortex structures and cavitation for wing configurations by technical solutions is fairly old. Besides the familiar aspects of classic propeller design, one may know for instance the propeller tip vane by Vatanabe [7], ducted tips or bulbous tips [6], to name but a few. With each solution having its individual benefits, it is obvious that application for retrofit becomes difficult, if cavitation characteristics and customers expectations does not comply.

In lights of this, the investigations of Katz and Galdo [4] pointed out a distinct relation between surface roughness and tip vortex roll-up for a rectangular hydrofoil, demonstrating a shift in detachment point and a substantial reduction in tip vortex strength due to increasing surface roughness. Based on these results, Johnsson and Ruttgerson [1] studied the influence of leading edge roughness on the tip vortex roll-up for different angles of attack. It was shown, that application of roughness on the pressure side near the leading edge has a delaying effect on tip vortex cavitation. On the downside of these results was an increase in drag up to 10% due to the highly exposed roughened area causing a total decrease in efficiency by 2%.

Philipp and Ninnemann [5] suggested, that small scale turbulence pertubation within the boundary layer, caused by surface roughness, may result in a destabilizing of the tip vortex structure. They claimed the back on the suction side of the propeller tip to be the most efficient application area. Cavitation tunnel experiments proved a scattered cavitating vortex structure and a decrease of 2^{nd} order pressure fluctuations of 35% accompanied by a lowering of open water efficiency of 2.5%.

An evidence for the connection between turbulence of the outer flowfield and vortex core dynamics was given by the work of Hussain and Pradeep [2], pointing out that the eigenmodes of the evolving vortex allow resonance effects with the relatively week outer turbulence leading to pertubation amplification by several orders of magnitude.

3 SETUP

3.1 Numerical Setup

A blade model based on the P1380 cavitation tunnel experiments of the Potsdam Model Basin was designed, providing an equal thrust distribution within translational flow as its rotational counterpart. Staying with the chord-, skew- and thickness distribution of the original P1380, the blade sections were straightened into horizontal plane. Using

symmetric sections, the original camber distribution was reset. The pitch distribution was found impressing the calculated thrust distribution $F_{A,des}$ of the original P1380 propeller to the translational model using a panel code for solving the equations

$$\Delta F_{A,j} = \left[F_{A,des,j} - \sum_{i=1}^{N} \left(\frac{\partial F_{A,j}}{\partial \alpha_i} \alpha_i \right) \right] \rightarrow 0 \tag{1}$$

$$\frac{\partial F_{A,i}}{\partial \alpha_i} = \frac{F_{A,i}\left(\alpha_{init} + \Delta\alpha_i\right) - F_{A,i}\left(\alpha_{init}\right)}{\Delta \alpha_i}$$

For optimal validation the blade model was scaled by a factor of 1:7.5, leading to a total span of b=445.5mm and a chord length of c(r/R=0.7)=412.7mm with a maximum thickness of t(r/R=0.7)=17.9mm.

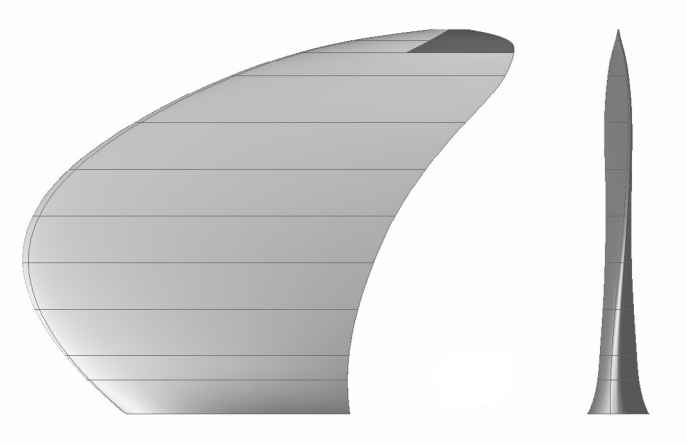

Figure 1: P1380 blade model for translational inflow with tip roughness

The computational domain consists of a block-structured ICEM grid using 19 Mio. as well as 60 Mio. hexahedron cells per blade. To ensure grid independent vortex development, the downstream section of the tip was set up with an equally spaced cartesian grid, resolving the vortex cross section by 56 x 56 and 331 x 331 cells respectively. Calculating the flowfield with the OpenFoam steady state RANS Solver SimpleFoam and a SST turbulence model, the wall function implementation of Tapia [8] was used to model different sizes of sand grain roughness $h_s^+ = h_s u_\tau / \nu$ in the transitional and the fully rough regime. Within the logarithmic profile

$$u^+ = \frac{1}{\kappa} \ln\left(y^+\right) + B - \Delta B \tag{2}$$

the velocity shift for the roughened wall reads

$$\Delta B = \frac{1}{\kappa} \ln\left[\frac{h_s^+ - 2.25}{87.75} + C_s h_s^+ \right]^{\sin\left(0.4258\left(\ln h_s^+ - 0.811\right)\right)} \qquad \text{for } 2.5 \leqslant h_s^+ \leqslant 90 \tag{3}$$

$$\Delta B = \frac{1}{\kappa} \ln\left(1 + C_s h_s^+\right) \qquad \text{for } h_s^+ \geqslant 90$$

The constant C_s, denoting the roughness type, was found in a series of calculation of the Nikuradse wall friction factor for turbulent pipe flows at Re=10^6, showing best overall prediction for C_s=0.35 (fig. 2).

According to [5] sand grain roughness elements of h_s=[0.2, 0.4, 0.6]mm has been considered for suction sided (SS), pressure sided (PS) and suction + pressure sided (SSPS) application areas of $0.95 \leqslant r/R \leqslant 1$ and $0.5 \leqslant c_L \leqslant 1$. The Reynolds-Number was set to Re=10^6 leading to an inlet velocity v_{inlet}=42.3m/s.

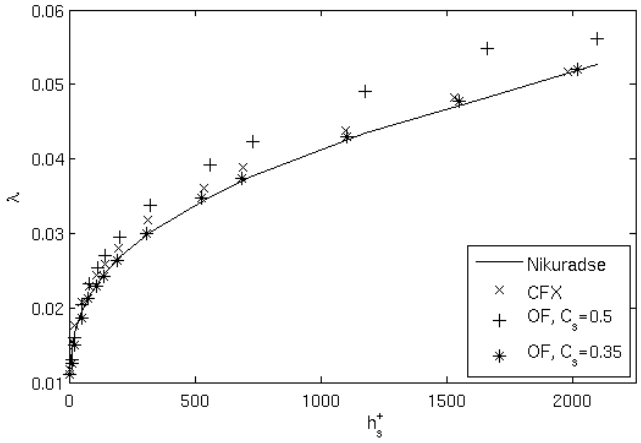

Figure 2: Wall function calculations for wall friction factor in turbulent pipe flows at Re=10^6

3.2 Experimental Setup

For validation purpose the pressure and the velocity field within the tip vortex for a smooth and a roughened wing were measured, showing the same dimensions as in the numerical setup. Two types of roughness structures had been investigated: Unstructured roughness, formed by a single layer of corundum with mean diameters of [0.2, 0.4, 0.6]mm in an adhesive matrix and structured roughness using adhesive stripes with a height of 0.6mm, width of 4.5mm and distance of 4.5mm. The stripes were placed in stream, cross-stream and diagonal direction. Structured roughness types were applied to the suction side of the tip only whereas the unstructured type was used either on suction or pressure side (tab. 1).

The measurement series was carried out at a Goettingen type subsonic wind tunnel, providing a quadratic measurement cross-section of $2m^2$. Integral forces and momentum on the blade model have been recorded by a six-component measurement system. To ensure matching of experimental and simulation data angle of attack and lift of the wing was selected representing the numerical data.

Within a vertical cross section perpendicular to the main inflow direction 0.5m downstream from the generator line with its center at 0.427 m vertical height 3D Hot-Wire as

well as Prandtl Tube measurements were performed. The cross section extended 165 mm x 165 mm being resolved as in the numerical setup by 56 x 56 measurement points.

4 RESULTS

4.1 Numerical Results

The simulations showed a distinct relation between roughness height and area of the tip roughness and specific tip vortex parameters. Applying sand grain roughness to the suction side of the tip, the viscous stresses between tip surfaces and adjacent tip vortex were increased, resulting in a damping of the angular momentum and therefore in an increased vortex pressure. The strong pattern of turbulent kinetic energy, forming above the roughened surface, quantifies the losses of rotational energy within the vortex. Depending on the investigated roughness height, the production rate of turbulent kinetic energy exceeds twice as much as for the smooth configuration. Even though the dissipation rate beeing enhanced as well, leading to an overall reduction of energy contained within the considered system, the turbulent scales dissipate imperfectly. Turbulent fragments tend to roll up into the vortex, shifting the relation between axial and radial cross stresses within the vortex core. For suction sided tip roughness all investigated heights leaded to an increased vortex core pressure compared to the smooth configuration. Due to additional viscous stresses the overall drag of the blade body rises, while the lift decreases.

Applying sand grain roughness to the pressure side, the tip vortex pressure and angular momentum remains nearly constant compared to the smooth wing, as the viscous effects and vortex are physically separated by the propeller blade. Acting on the boundary layer, the roughened region virtually thickens the blade section in the tip area, increasing the lift slightly. The drag of this configuration is larger than for the smooth wing and for the suction sided roughened wing as well.

Suction and pressure sided tip covered with sand grain roughness show a comparable impact on angular momentum and tip vortex pressure as for the suction sided configuration. Drag and lift nearly superposition from the single sided types, leading to the highest drag of all investigated configurations where lift decreases slightly compared to the smooth wing.

Calculating the inverse of the glide ratio ε, one can obtain a decrease in wing efficiency for all setups. These effects become stronger for all configurations as the roughness height increases (fig. 4).

As the wall roughness thickens the boundary layer, the correlation between boundary layer thickness of the wing and tip vortex diameter, like mentioned in [9], was investigated. The tangential vortex velocity at one chordlength downstream of the generator line was compared for the smooth, the suction sided and the pressure sided tip roughness. In addition three more cases were calculated: The complete blade covered with roughness (allrough), providing a thickened boundary layer, the complete blade set up with a no-slip condition (allslip), inhibiting the development of a boundary layer, and a no-slip condition

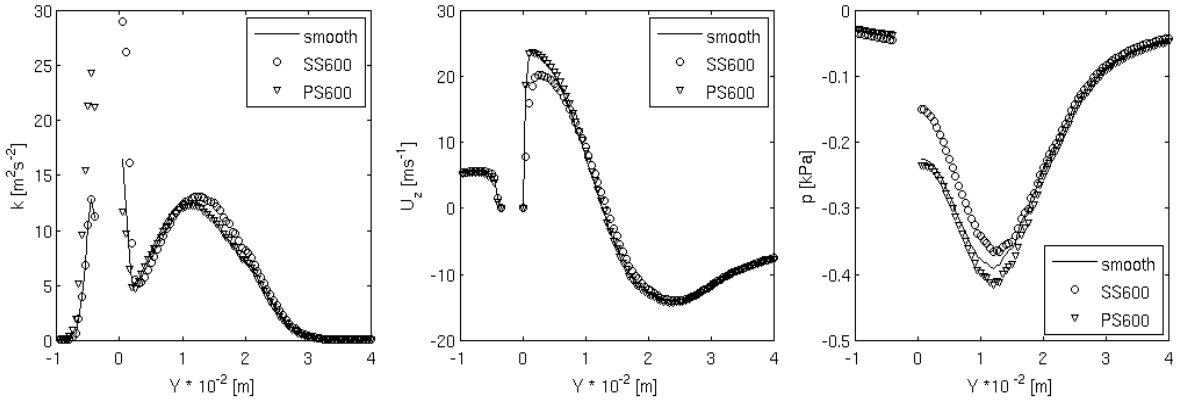

Figure 3: Calculated turbulent kinetic energy (left) tangential velocity (center) and pressure (right) on a horizontal line through the tip vortex adjacent to the roughness patch

for the suction side of the tip only (SSslip), inhibiting the thickening of the boundary layer at the tip.

In the outcome no dependency of the tip vortex diameter on boundary layer thickness was found. Comparing the circumferencal velocities, normed by the lift coefficient, all configurations showed a similar relation between specific lift and vortex circulation, except for two configurations: The suction side roughened blade and the entirely roughened blade as well presented a significant decrease in tangential vortex velocity within a radii of $R \leq 2R_{\text{solid}}$ and subsequently an increase in tip vortex pressure. Even though the entirely covered blade show superior vortex characteristics, it exhibits an essential increase in viscous friction (+85.6%) and therefore reduction of blade efficiency (-73.0%), whereas the suction sided provides nearly the same resistance (+0.4%) and efficiency (-0.9%) as for the smooth blade.

To investigate the effects of turbulent structures, the reynolds stresses, evolving at the roughened patches, were mapped either onto the suction side or the pressure side of the smooth propeller tip. In contrast to the expectations, no influence on the tip vortex pressure has been observed. The turbulent scales roll up into the vortex, traveling downstream within the vortex core.

4.2 Experimental Results

The calculations were assisted by a series of wind tunnel measurements, proving the low-pressure region of the tip vortex being effected by the tip roughness depeding on the applicaton area. Where for the suction sided tip roughness an increase of up to 18.4% was measured, the pressure sided tip roughness seems to have only marginal effect on the vortex vacuum. This is surprising somehow, since the measurements showed a significant decrease of the axial velocity surpression within the vortex core for both roughness

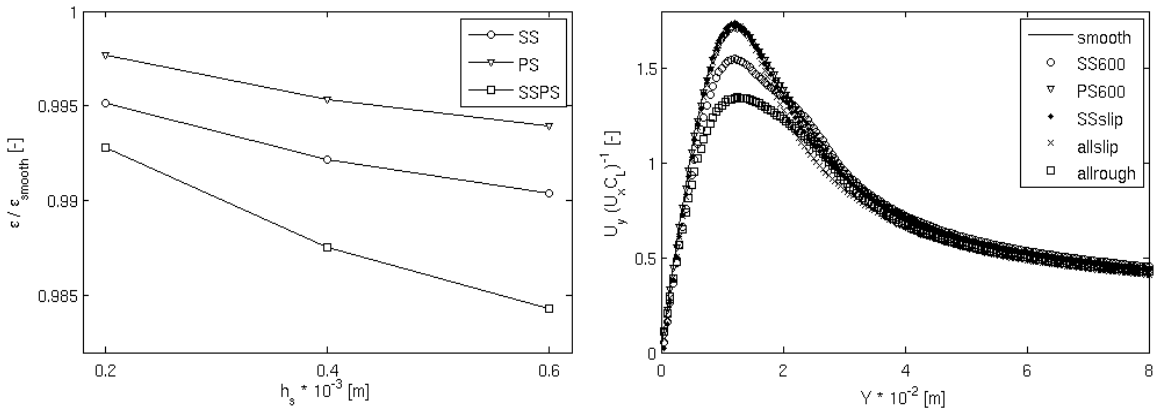

Figure 4: Calculated blade efficiency relative to a smooth wing depending on roughness height and application area (left) and tangential vortex velocity one choordlength downstream of the propeller blade

configurations, with an even stronger effect of the pressure sided tip roughness (SS600: -11.1%/-8.6%; PS600: -31.1%/-23.3% (Prandtl tube/3D Hotwire)). As indicated by the simulation results, the effect of suction side roughness on the tip vortex vacuum correlates with the roughness height. This is true for the unstructured roughness type only, since all structured roughness setups showed to have less impact on the vortex vacuum than the smallest sand grain height, even though this sand grain roughness extends only one third of the structured type. While all structured types provided the same roughness height, their sensitivity regarding the inflow direction became obvious. Whereas the horizontal stripes showed to have the least impact on the tip vortex vacuum from all suction sided measures, the diagonal stripes, aligning perpendicular to the resulting inflow direction of mean flow and vortex rotation, proved to be nearly as effective as the smallest unstructured height.

Table 1: Investigated roughness types

	tip area	type	height	$(p/p_{smooth})_{RANS}$	$(p/p_{smooth})_{Exp}$
SS200	suction side	sand grain	0.2mm	0.974	0.864
SS400	suction side	sand grain	0.4mm	0.939	0.822
SS600	suction side	sand grain	0.6mm	0.905	0.816
PS600	pressure side	sand grain	0.6mm	1.023	0.969
SSHoriz	suction side	horizontal stripe	0.6mm	-	0.903
SSVert	suction side	vertical stripe	0.6mm	-	0.940
SSDiag	suction side	diagonal stripe	0.6mm	-	0.870

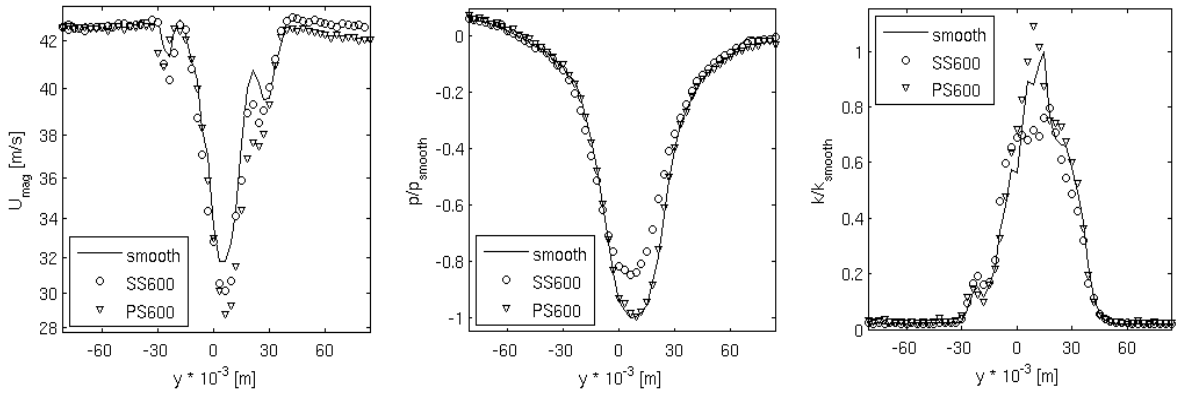

Figure 5: Dynamic pressure (left), static pressure (center) and turbulent kinetic energy (right) for a smooth and a roughened wing (h_s=600μm) on a horizontal line through the vortex core (distance from generator line x=0.35m, z=0.427m)

Comparing the second order moments for the suction side roughness, a diffusion of the turbulent kinetic energy is observed, thickening the turbulent vortex core (fig. 5). By a closer look at the diagonal Reynolds stresses, an amplification of the axial vortex stresses can be noticed, whereas the radial stresses seem to be diminished. Taking into account that for the given configuration the axial stresses averaging at 1/3 of the radial stresses, the vortex diffusion can be divided into two fractions: First, a thickening of the vortex core by an amplification of the axial stresses, and second, the lowering of the total kinetic energy within the core by damping the radial stresses (fig. 6). The shifting relation between axial and radial core stresses is also reflected by the experimental data for the cross-correlations, showing an amplification of the correlations between axial and radial fluctuations in opposite to the damping of the correlations between both components of the radial fluctuations.

As the pressure sided roughness showing a similar amplification of the axial stresses, in this case the radial stresses are amplificated as well, leading to an overall increase of the turbulent kinetic energy within the vortex core. This is in line with the results observed for the radial cross stresses, being enhanced by the pertubation of the vortex roll up in vicinity of the tip, evidencing a more turbulent vortex structure compared to all other configurations.

5 CONCLUSIONS

The effects of propeller tip roughness and application area on the tip vortex pressure had been investigated. It was shown that the tip vortex vacuum can be reduced using suction sided tip roughness. Although the impact on the vortex vacuum was suggested by the calculations, an even stronger influence of the roughened tip on the low-pressure region of the tip vortex was measured. This effect originates from increased viscous wall-friction

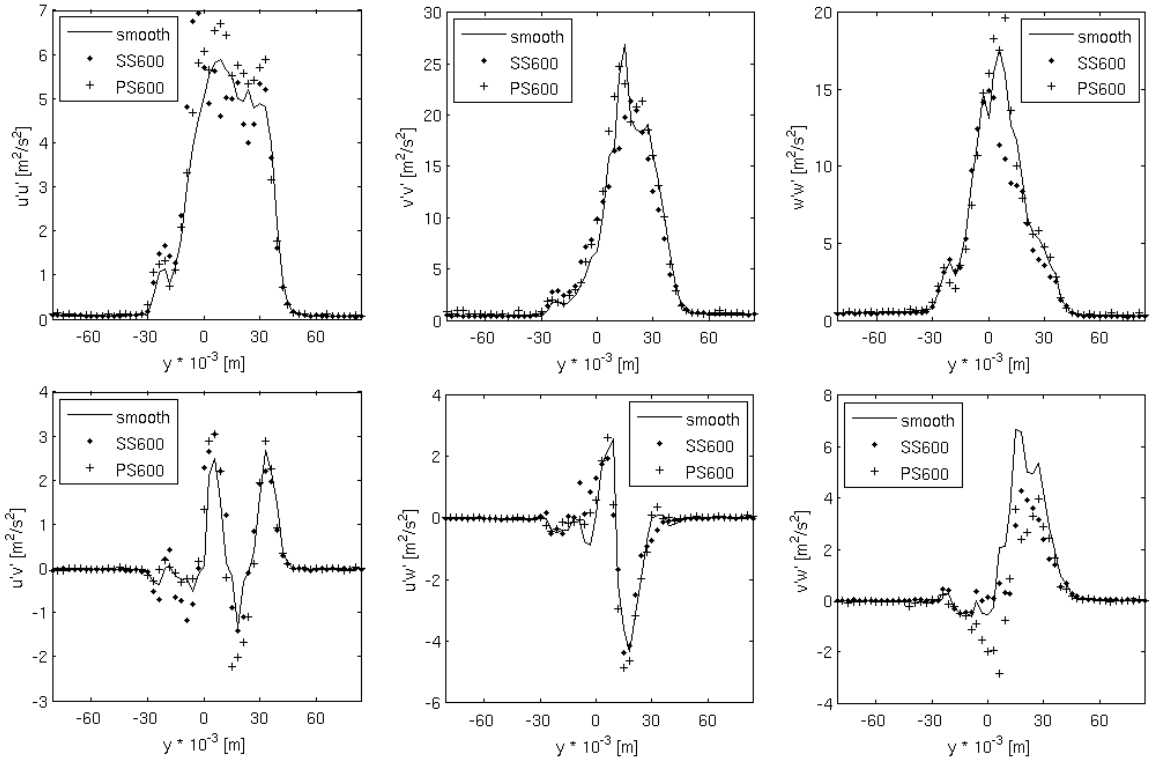

Figure 6: Components of the Reynolds stress tensor for a smooth and a unstructured roughened wing (h_s=600μm) on a horizontal line through the vortex core (distance from generator line x=0.4806m, z=0.427m)

between the vortex and the roughened tip, damping the circumferencal vortex velocity. Considering the suction sided sand grain roughness to be the most effective solution within this investigation, the structured roughness, even though being sensitive regarding the inflow direction, also showed promising potential for vortex pressure modification. Due to the basic design this version seems to be most preferable for practical application. It can be estimated that by minimized reduction of the open water efficiency due to friction induced losses, cavitation safety in the tip vortex can be improved by up to 19%.

As this study is concentrated on the physical effects within one-phase flows in the first, all results are going to be validated during the second phase of the project in cavitation tunnel experiments for the rotational propeller model. At the present state of the investigation it can be expected, that the specific application of discrete roughness structures near the propeller tips offers potential to efficient propulsion systems that meets highest industries demands for cavitation-free operation.

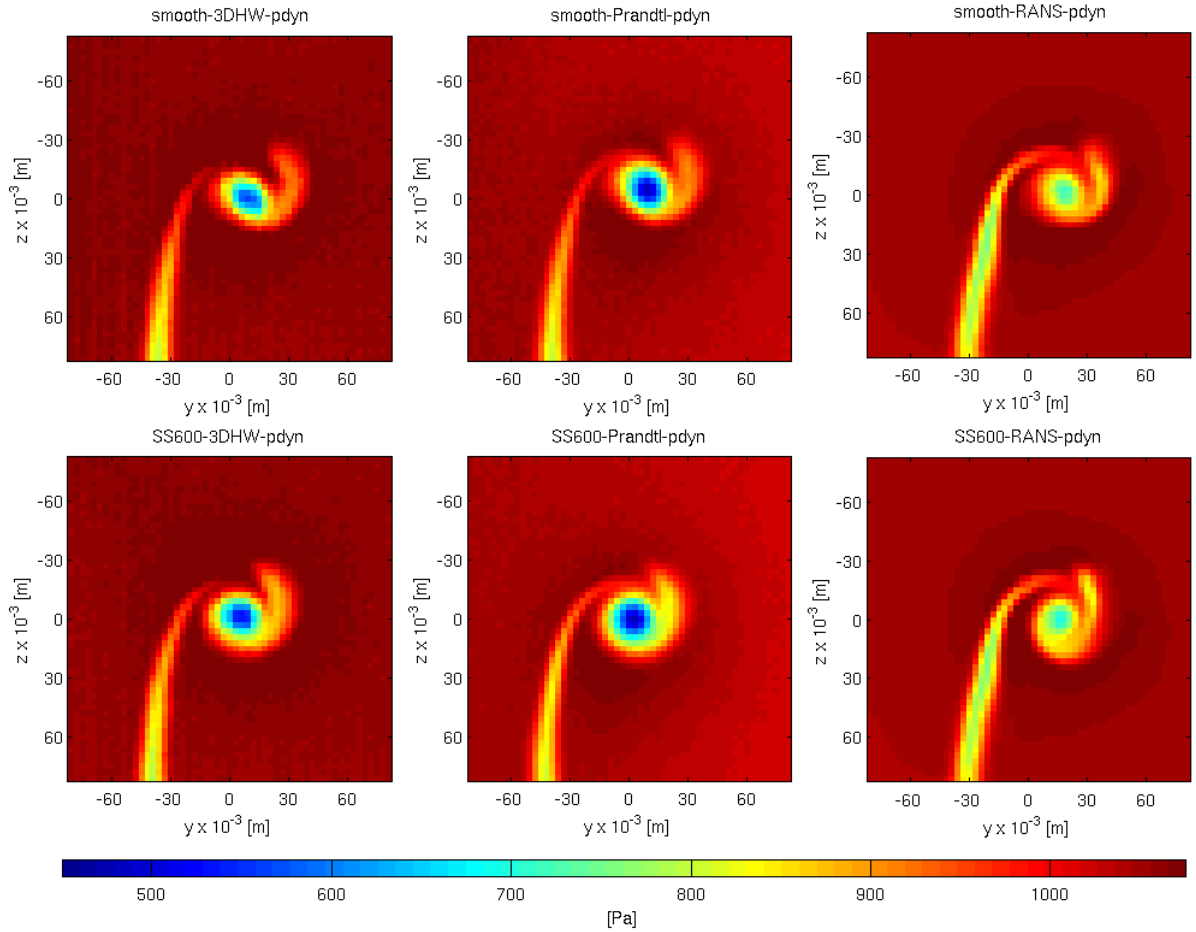

Figure 7: Dynamic pressure from 3D Hot Wire (left), Prandtl Tube (middle) and RANS (right) behind a smooth (top) and a roughened (bottom) propeller tip

REFERENCES

[1] O. Rutgerson C. A. Johnsson. Leading edge roughness - a way to improve propeller tip vortex cavitation. *Propellers and Shafting Symposium*, 1991.

[2] D. S. Pradeep F. Hussain. Mechanism of core pertubation growth in vortex-turbulence interaction. *12th Asian Congress of Fluid Mechanic*, 2008.

[3] A. Junglewitz J. Friesch. Erocav - improved test methods based on full scale investigations and new theoretical approaches for the prediction of erosion damages. *Summer Meeting STG*, 2003.

[4] J. Galdo J. Katz. Effect of roughness on rollup of tip vortices on a rectangular hydrofoil. *Journal of Aircraft*, 26, 1989.

[5] P. Ninnemann O. Philipp. Wirkung von fluegelrauigkeiten auf kavitation und erregung. 2007.

[6] S. Z. Duan S. I. Green. The ducted tip - a hydrofoil tip geometry with superior cavitation performance. *Journal of Fluids Engineering*, 117, 1995.

[7] H. S. Koyama T. Watanabe, H. H. Nigim. The effects of propellertip vane on flow-field behavior. *Experiments in Fluids*, 23, 1997.

[8] X. P. Tapia. Modelling wind flow over complex terrain using openfoam. 2009.

[9] S. I. Liapis G. J. Follin W. J. Devenport, M. C. Rife. The structure and development of a wingtip vortex. *Journal of Fluid Mechanics*, 312, 1996.

[10] D. Wittekind. Current status of underwater noise from shipping and the contribution of the propeller. 2011.